Bioorg. Med. Chem. Lett. 125–126 (2025) 130282

Contents lists available at ScienceDirect

Bioorganic & Medicinal Chemistry Letters

journal homepage: www.elsevier.com/locate/bmcl

Design and structural optimization of novel SOS1 inhibitors in KRAS-driven cancers

Yating Chen [a,1], Qiupei Liu [c,e,1], Xianghui Meng [f], Wenxu Cao [c,d], Lihui Duo [e], Xiaorong Song [b], Xiangchun Shen [a], Sze Shin Low [e], Wan Yong Ho [g], Bencan Tang [e,**], Pengli Zhang [b,**], Hua Xie [b,c,d,*], Guoqin Xia [a,b,c,d,f,*]

[a] State Key Laboratory of Discovery and Utilization of Functional Components in Traditional Chinese Medicine, School of Pharmaceutical Sciences, Guizhou Medical University, Guiyang 550014, China
[b] Zhongshan Institute for Drug Discovery, Shanghai Institute of Materia Medica, Chinese Academy of Sciences, Zhongshan 528400, China
[c] Shanghai Institute of Materia Medica, Chinese Academy of Sciences, Shanghai 201203, China
[d] University of Chinese Academy of Sciences, Beijing 101408, China
[e] Faculty of Science and Engineering, The University of Nottingham Ningbo China, Ningbo 315100, China
[f] School of Chinese Materia Medica, Nanjing University of Chinese Medicine, Nanjing 210000, China
[g] Faculty of Medicine and Health Sciences, University of Nottingham Malaysia, Semenyih 43500, Malaysia

ARTICLE INFO

Keywords:
SOS1 inhibitor
KRAS mutation
SOS1-KRAS interaction
Resistance

ABSTRACT

The development of small molecular inhibitors to target the guanine nucleotide exchange factor SOS1 has been proved to be a hopeful strategy for the treatment of various KRAS-driven cancers. Constructing novel SOS1 inhibitors is urgently needed due to the increasing drug resistance arising from structural similarity of earlier analogs. Herein, we discovered a new SOS1 inhibitor with para-dimethylaminoazetidine quinazoline scaffold. The most potent compound 10i showed superior activity to the reported SOS1 inhibitor Hit 1 in both the KRASG12C::SOS1 PPI inhibition assay and 3D proliferation inhibitory assay, and compound 10i presented enhanced aqueous solubility under physiologically relevant pH 6.8. Moreover, compound 10i could down-regulate the levels of phosphorylated ERK and AKT in the NCI-H358 cancer cell line. Overall, these studies showed that 10i was a promising drug candidate for the treatment of KRAS-driven cancer.

KRAS (Kirsten rat sarcoma viral oncogene homologue) is one of the most frequently mutated oncogenes in human cancers, driving tumorigenesis in approximately 25 % of all malignancies, including pancreatic ductal adenocarcinoma (PDAC, >90 %), colorectal cancer (CRC, ~45 %), and non-small cell lung cancer (NSCLC, ~30 %).[1–3] Despite its well-established role in cancer progression, KRAS has long been considered "undruggable" due to its smooth surface and high affinity for GTP, which makes it challenging to design effective small-molecule inhibitors.[4] The first major milestone in KRAS drug development was the discovery of covalent inhibitors targeting the $KRAS^{G12C}$ mutation, which accounts for a significant subset of KRAS-driven cancers.[5] Covalent inhibitors such as sotorasib (AMG 510) and adagrasib (MRTX849) have demonstrated remarkable clinical efficacy by selectively binding to the inactive, GDP-bound form of $KRAS^{G12C}$ and trapping it in an inactive state.[6–9] These inhibitors have shown promising results in clinical trials, leading to the FDA approval of sotorasib in 2021 for the treatment of $KRAS^{G12C}$-mutated NSCLC, and this breakthrough has validated KRAS as a druggable target.[10,11] However, marketed $KRAS^{G12C}$ inhibitors are ineffective against non-G12C mutations (e.g. G12D, G12V, G13D), which represent the majority of KRAS-driven cancers.[12–14] Additionally, resistance mechanisms, such as adaptive feedback signaling and secondary KRAS mutations, have emerged as critical barriers to the long-term efficacy of these therapies.[15,16] These limitations and unmet medical need have spurred efforts to develop next-generation KRAS inhibitors, especially pan-KRAS inhibitors.

Beyond direct KRAS inhibition, alternative strategies targeting

* Corresponding authors at: Zhongshan Institute for Drug Discovery, Shanghai Institute of Materia Medica, Chinese Academy of Sciences, Zhongshan 528400, China.
** Corresponding authors.
E-mail addresses: bencan.tang@nottingham.edu.cn (B. Tang), zhangpengli@zidd.ac.cn (P. Zhang), hxie@simm.ac.cn (H. Xie), xiaguoqin@simm.ac.cn (G. Xia).
[1] The author contributed equally to this work

https://doi.org/10.1016/j.bmcl.2025.130282
Received 19 March 2025; Received in revised form 13 May 2025; Accepted 14 May 2025
Available online 16 May 2025

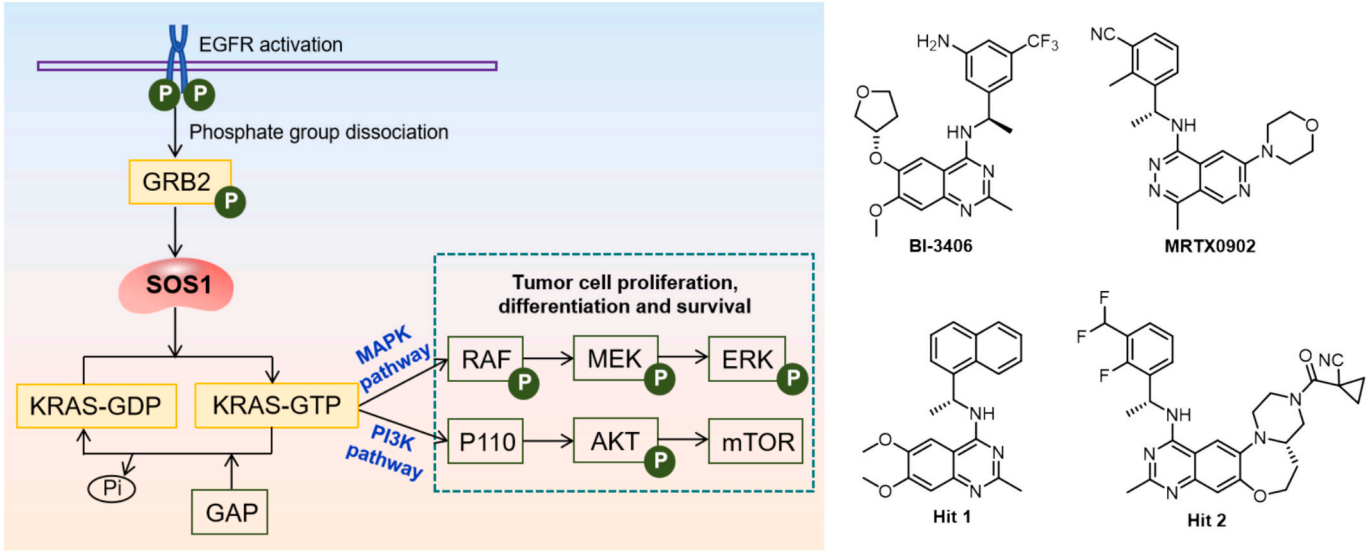

Fig. 1. The KRAS signaling pathway regulated by SOS1 and some representative SOS1 inhibitors.

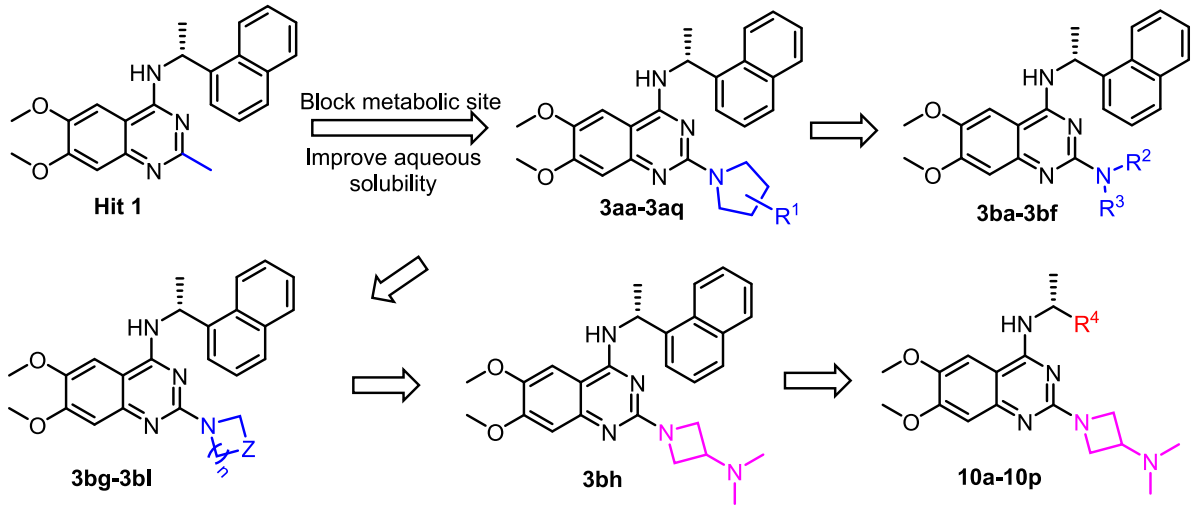

Fig. 2. Structural optimization of target compound.

upstream regulators and downstream effectors of the KRAS signaling pathway to overcome certain types of drug resistance are being actively explored.[17,18] These approaches aim to disrupt KRAS signaling indirectly and provide therapeutic options for patients with diverse KRAS mutations. Among these regulators/effectors, Son of Sevenless 1 (SOS1), a guanine nucleotide exchange factor (GEF), has emerged as a promising therapeutic target and plays a critical role in activating KRAS by catalyzing the exchange of GDP for GTP.[19–21] In KRAS-mutant cancers, SOS1-mediated activation of KRAS is often dysregulated, leading to sustained oncogenic signaling and uncontrolled cell proliferation.[22] Preclinical studies have demonstrated that SOS1 inhibition can effectively suppress KRAS signaling and impair tumor growth, highlighting its potential as a therapeutic strategy (Fig. 1).[23–25] However, existing SOS1-targeting compounds face challenges such as limited potency, poor pharmacokinetic properties, or acquired resistance due to feedback mechanisms.[26] Thus, there is a pressing need for more potent, selective, and clinically viable SOS1 inhibitors. In this paper, we described the discovery of the *para*-dimethylamino-azetidine quinazoline scaffold for efficaciously disrupting the SOS1 – KRAS interaction, and our lead compound 10i displayed nanomolar IC_{50} to inhibit SOS1 – KRAS protein-protein interaction.

Most currently developed SOS1 inhibitors feature a methyl group at the 2-position of the quinazoline scaffold. To block metabolic site and enhance aqueous solubility, we conducted structural optimization based on the SOS1 inhibitor Hit 1 by replacing the methyl group with nitrogen-containing moiety, aiming to identify novel compounds with improved solubility profiles and high potency (Fig. 2). The reference compounds Hit 1 and BI-3406, established reference agents in SOS1 inhibitor research, served as benchmark compounds in the comparative evaluation. The synthetic routes for target compounds were detailed in Schemes S1 – S3 (Supporting Information). We initially focused on modifying the hit compound Hit 1 by replacing its methyl group with tetrahydropyrrole ring. Regrettably, all tetrahydropyrrole-substituted derivatives (3aa–3aq) exhibited a significant reduction in SOS1 – KRAS PPI inhibitory activity compared to Hit 1 in Table 1, suggesting that inappropriateness of tetrahydropyrrole ring at this position compromised target engagement. We next explored the effects of introducing aliphatic chains and other aliphatic heterocycles on inhibitory activity. As shown in Table 2, structural modifications at the 2-position of the quinazoline core revealed that methylamine and dimethylamine derivatives (3ba and 3bd) in aliphatic chain derivatives 3ba–3bf performed acceptable inhibition rates (IR) at 1 μM. Among

Table 1
Structures and inhibition rates at 1 μM of 3aa-3aq with different R^1.

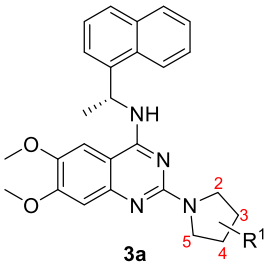

3a

Compd.	R^1	HTRF KRAS::SOS1 PPI inhibition at 1 μM	Compd.	R^1	HTRF KRAS::SOS1 PPI inhibition at 1 μM
3aa	–	37.4 ± 1.2	3aj	(S) 3-NH_2	27.4 ± 0.7
3ab	(S) 2-CH_3	9.3 ± 0.7	3ak	(R) 3-NH_2	40.4 ± 0.3
3 ac	(R) 2-CH_3	16.0 ± 0.4	3al	(S) 3-$NHCH_3$	23.9 ± 3.0
3ad	(S) 3-CH_3	16.5 ± 0.5	3 am	(R) 3-$NHCH_3$	25.5 ± 0.7
3ae	(R) 3-CH_3	22.8 ± 2.7	3an	(S) 3-N$(CH_3)_2$	24.7 ± 3.7
3af	(S) 2-CH_2OH	25.0 ± 1.3	3ao	(R) 3-N$(CH_3)_2$	28.9 ± 0.5
3ag	(R) 2-CH_2OH	15.6 ± 0.4	3ap	(S) 3-F	20.2 ± 1.9
3ah	(S) 3-OH	20.4 ± 1.5	3aq	(R) 3-F	31.6 ± 2.6
3ai	(R) 3-OH	40.3 ± 0.0	Hit 1	/	81.2 ± 1.2

KRAS::SOS1 PPI, KRAS(G12C)::SOS1 PPI; Inhibition rates were shown as the mean ± SD from three replicate experiments.

aliphatic heterocycle derivatives 3bg–3bl, compound 3bg featuring azetidine and compound 3bh bearing *para*-dimethylamino-azetidine exerted potential inhibition rates on SOS1 − KRAS PPI (IR = 49.6 %, 56.2 %, respectively). Inspired by these results, we fixed the 2-position as the *para*-dimethylamino-azetidine moiety and systematically optimized the replacement of naphthalene ring (Table 3). When the replacement of naphthalene ring with heterocycles (thiophene, furfuran, quinoline, benzothiophene and benzofuran), compounds 10 l − 10p exhibited limited potency in disrupting SOS1-KRAS PPI (IR < 20 %). Among phenyl derivatives 10a − 10 k, compound 10 h (containing a 3-difluoromethyl-2-fluorophenyl group) exhibited an IR of 73.1 %, and compound 10i (containing a 3-amino-5-(trifluoromethyl)phenyl group) displayed the highest inhibition rate (IR = 83.8 %), which was superior to Hit 1.

To further evaluate the potential of compound 10i containing a *para*-dimethylamino-azetidine moiety, compound 12 with methyl group was synthesized (Fig. 3A). The inhibitory activities of compounds 10i, 12, Hit1 and BI-3406 against the KRAS::SOS1 PPI were assessed, and the aqueous solubilities at pH = 2 and pH = 6.8 were also determined (Fig. 3B and C).[27] Notably, compound 10i exhibited comparable inhibitory potency (IC_{50} = 165.2 ± 13.8 nM) to its methyl counterpart 12 (IC_{50} = 126.3 ± 15.9 nM), and was superior to that of Hit1 (IC_{50} = 238.7 ± 6.1 nM). Although BI-3406 demonstrated superior PPI inhibition relative to 10i, the latter displayed significantly enhanced aqueous solubility under weakly acidic condition (pH = 6.8) (Fig. 3C). This improvement in aqueous solubility at physiologically relevant pH suggested that the *para*-dimethylamino-azetidine moiety conferred favorable ionization properties, potentially enhancing drug absorption-a critical pharmacokinetic advantage for therapeutic candidates targeting intracellular PPIs.

A molecular simulation study also provided a similar binding mode of the newly synthesized compounds 10 h and 10i when compared with BI-3406. As shown in Fig. 4, in 10 h-SOS1 complex, the quinazoline core of compound 10 h and benzene ring in 3-(difluoromethyl)-2-fluorophenyl)ethyl fragment could form the π − π stacking interaction, and the N atom of quinazoline core could form hydrogen bond with GLU-902 residue. In 10i-SOS1 complex, the quinazoline core orientated in a parallel position with His-905 and formed the π − π stacking interaction, and additional hydrogen bonds formed by the H atoms of two amino groups in 3-amino-5-(trifluoromethyl)phenylethan-1-amine fragment with O atoms in ASN-879 and MET-878 residues respectively were observed. The extended network of stable hydrogen bonds and other non-covalent effects helped to stabilize 10 h-SOS1 and 10i-SOS1 complexes, inducing strong affinities of 10 h and 10i with SOS1 protein.

To evaluate the antiproliferative effects of the SOS1 inhibitors, we employed a 3D cell viability assay to assess the growth-inhibitory activity of selected compounds 10 h and 10i against $KRAS^{G12C}$-mutant NCI-H358 lung cancer cell line (Fig. 5A).[28] As observed with the reported SOS1 inhibitor Hit 1, the tested compounds 10 h and 10i exerted excellent antitumor activities against NCI-H358 cell with IC_{50} values of 4.22 μM and 3.15 μM respectively, which were superior to the Hit 1 (IC_{50} = 8.45 μM). To further validate the antitumor potential of 10i at the cellular level, we conducted a cell colony formation assay to evaluate the long-term effect of the most promising compound 10i on the proliferative capacity of NCI-H358 cells. As demonstrated in Fig. 5B, 10i treatment resulted in a marked, concentration-dependent reduction in colony formation, indicating that compound 10i significantly suppressed the proliferative ability and population dependent growth of cancer cells.

To investigate the molecular mechanisms by which 10i suppresses NCI-H358 cell proliferation, we performed Western blot analysis to examine the activation status of key downstream signaling pathways regulated by KRAS, including the RAF-MEK-ERK and PI3K-AKT-mTOR cascades (Fig. 5C).[29] Compound 10i treatment led to a marked dose-dependent reduction in the phosphorylation levels of ERK1/2 (p-ERK, Thr202/Tyr204, extracellular signal-regulated kinase) and phosphorylated AKT (p-AKT, Ser473, protein kinase B) compared to the DMSO control group, while total ERK and AKT levels remained unchanged. Collectively, these findings highlighted the substantial potential of compound 10i as a SOS1 inhibitor to combat KRAS-mutant cells.

An ADMET study was carried out using SwissADME and pkCSM online softwares for predicting the drugability and pharmacokinetic properties of compounds 10 h and 10i (Table S1). 10 h and 10i complied with the Lipinski rule and had the same bioavailability score as Hit 1 and BI-3406. Moreover, compound 10i showed a theoretical negative response for blood–brain barrier (BBB) criteria and III category acute oral toxicity.

In summary, we here reported the discovery of 10i as a promising candidate compound for developing anti-KRAS drugs. Structure-based optimization of Hit 1 to 10p indicated that *para*-dimethylamino-azetidine quinazoline could serve as a potent scaffold for SOS1 inhibition. Systematic structural modification and activity evaluation led to the identification of compound 10i with excellent activity and enhanced aqueous solubility under physiologically relevant pH 6.8 when compared with the parental compound Hit 1. In vitro, SOS1 inhibition and theoretical results indicated that *para*-dimethylamino-azetidine ring was favorable, and a similar binding mode of compound 10i was observed when compared with BI-3406. Notably, compound 10i also induced dose-dependent inhibition of the phosphorylation level of the KRAS downstream signaling pathway proteins, ERK and AKT. Moreover, we found that compound 10i could suppress the proliferative ability and population dependency of NCI-H358 tumor cells. Given its optimized chemical structure and potent biological activity, 10i holds significant potential for further development as SOS1 inhibitor in the treatment of KRAS-mutant cancer cells.

Table 2
Structures and inhibition rates at 1 μM of 3ba-3bl with different R^2.

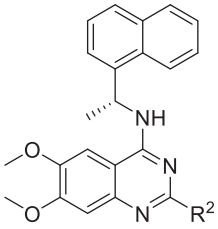

3b

Compd.	R^2	HTRF KRAS::SOS1 PPI inhibition at 1 μM	Compd.	R^2	HTRF KRAS::SOS1 PPI inhibition at 1 μM
3ba		46.0 ± 2.0	3bg		49.6 ± 1.5
3bb	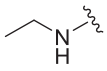	23.3 ± 7.7	3bh	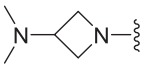	56.2 ± 1.8
3bc	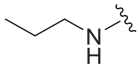	13.0 ± 2.6	3bi	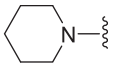	21.6 ± 3.0
3bd		55.2 ± 2.9	3bj	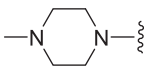	29.9 ± 1.8
3be	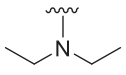	23.4 ± 6.3	3bk	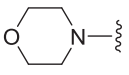	16.6 ± 1.5
3bf	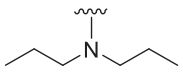	4.6 ± 1.5	3bl	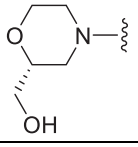	−0.7 ± 0.5

Table 3
Structures and inhibition rates at 1 μM of 10a-10p with different R^3.

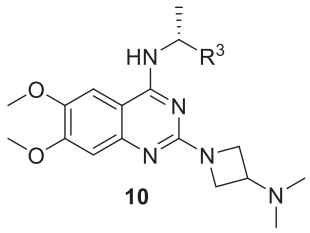

Compd.	R^3	HTRF KRAS::SOS1 PPI inhibition at 1 μM	Compd.	R^3	HTRF KRAS::SOS1 PPI inhibition at 1 μM
10a	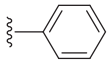	9.7 ± 0.5	10i	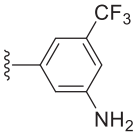	83.8 ± 0.6
10b	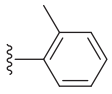	2.8 ± 0.8	10j	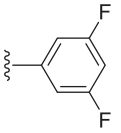	−1.6 ± 0.8
10c	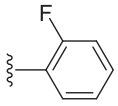	23.2 ± 3.2	10 k	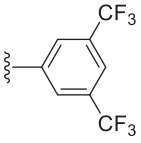	−14.9 ± 1.6
10d	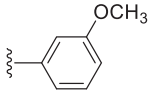	18.8 ± 1.8	10 l	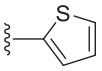	−11.5 ± 9.5
10e	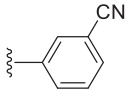	39.2 ± 1.7	10 m		−3.3 ± 3.1
10f	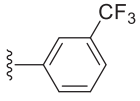	63.3 ± 0.1	10n	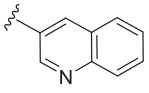	−5.8 ± 1.4
10 g	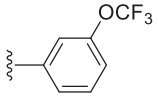	24.5 ± 1.6	10o	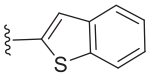	15.1 ± 0.5
10 h	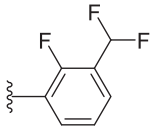	73.1 ± 0.3	10p	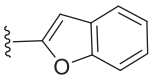	13.1 ± 1.4

A

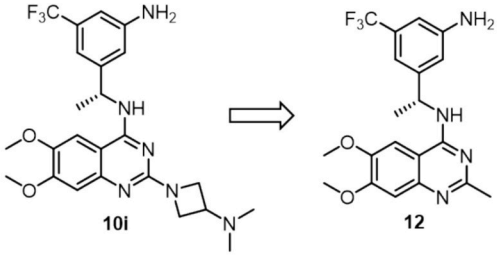

B

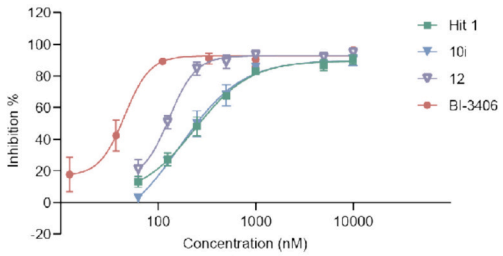

C

Compounds	HTRF KRAS::SOS1 PPI assay	Aqueous solubility (mg/mL)	
	IC_{50} (nM)	pH = 2	pH = 6.8
10i	165.2±13.8	0.647±0.035	0.567±0.083
12	126.3±15.9	0.500±0.047	0.045±0.005
Hit 1	238.7±6.1	0.068±0.002	< 0.025
BI-3406	41.9±3.7	0.673±0.050	0.060±0.008

Fig. 3. (A) Structural comparison of compound 10i to compound 12; (B) the inhibition of compounds 10i, 12, Hit 1 and BI-3406 against SOS1-mediated $KRAS^{G12C}$ activation by HTRF assay; (C) the IC_{50} values of compounds 10i, 12, Hit 1, BI-3406 in KRAS::SOS1 PPI assay and the aqueous solubility at pH = 2 and pH = 6.8.

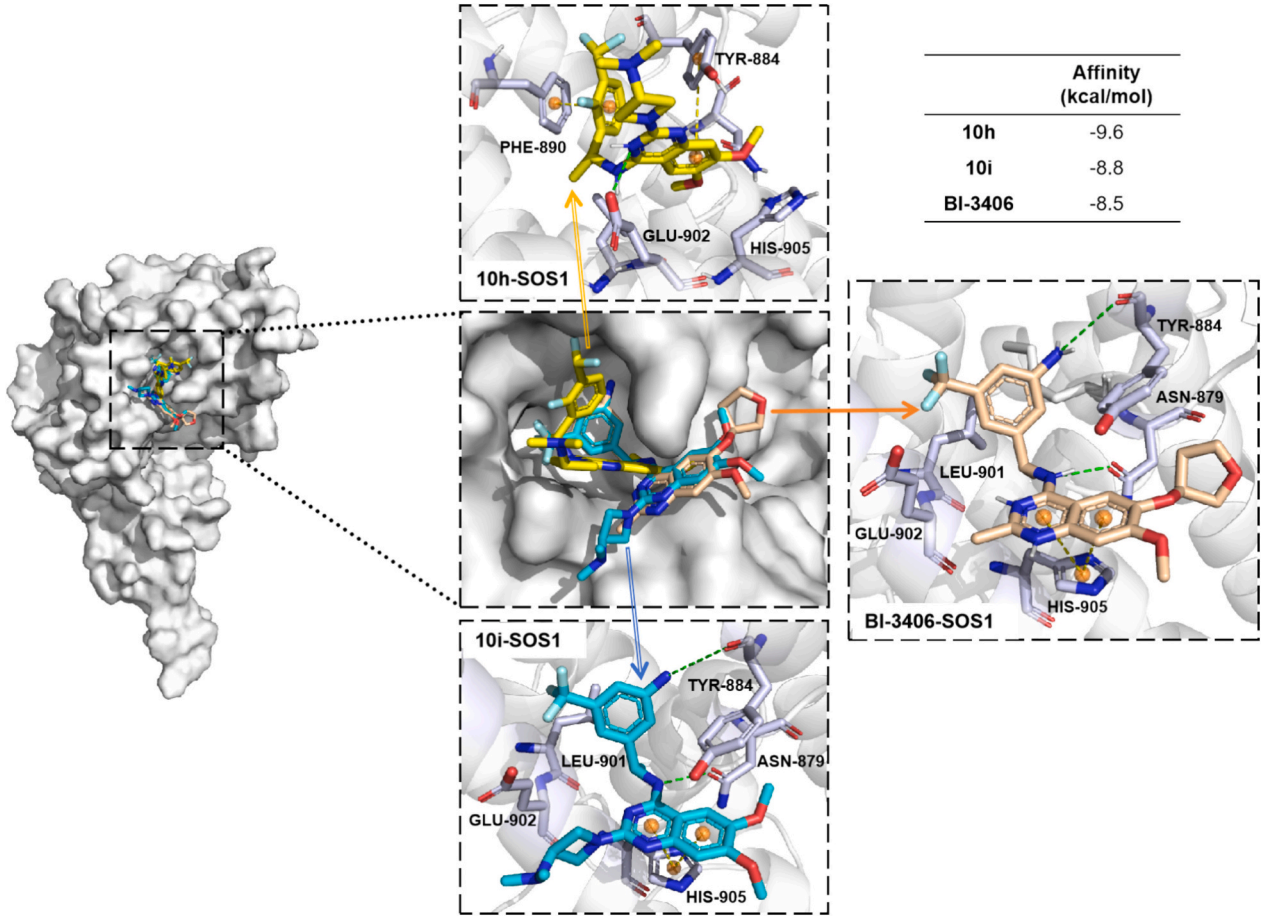

	Affinity (kcal/mol)
10h	-9.6
10i	-8.8
BI-3406	-8.5

Fig. 4. Modeled binding poses of 10 h, 10i and BI-3406 in SOS1 (PDB: 6SCM).

CRediT authorship contribution statement

Yating Chen: Investigation, Formal analysis, Data curation. **Qiupei Liu:** Investigation, Data curation. **Xianghui Meng:** Data curation. **Wenxu Cao:** Formal analysis, Data curation. **Lihui Duo:** Software, Data curation. **Xiaorong Song:** Investigation. **Xiangchun Shen:** Supervision. **Sze Shin Low:** Supervision. **Wan Yong Ho:** Supervision. **Bencan Tang:** Supervision. **Pengli Zhang:** Writing – original draft, Supervision,

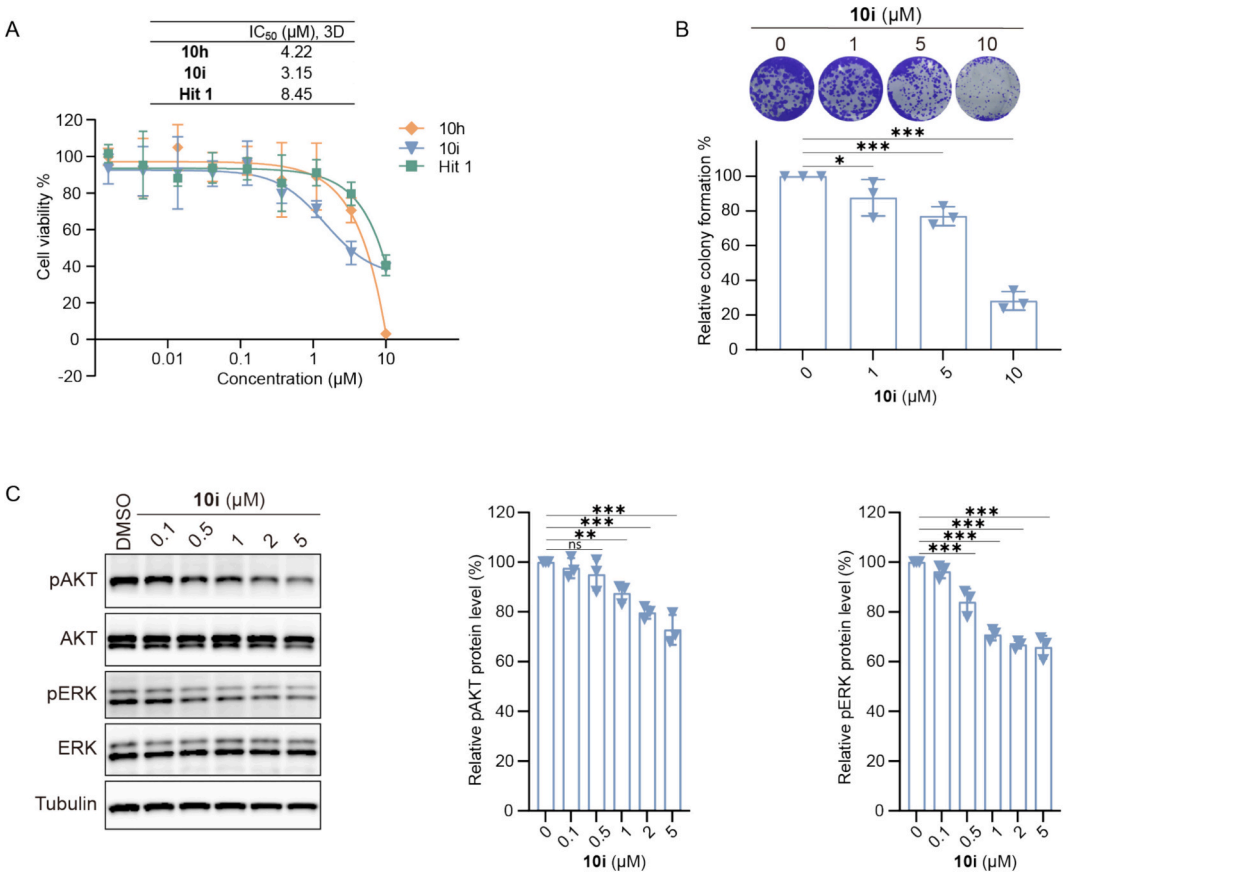

Fig. 5. (A) 3D proliferation inhibitory activities of 10 h, 10i and Hit 1 in NCI-H358 cell; (B) cell colony formation treated by 10i; (C) relative protein levels in NCI-H358 cell treated by 10i.

Formal analysis, Data curation, Conceptualization. **Hua Xie:** Writing – review & editing, Supervision, Funding acquisition. **Guoqin Xia:** Writing – review & editing, Supervision, Funding acquisition, Conceptualization.

Declaration of competing interest

The authors declare that they have no known competing financial interests or personal relationships that could have appeared to influence the work reported in this paper.

Acknowledgments

We gratefully acknowledge the Zhongshan Science and Technology Bureau (CXTD2023009), the Program for Young Talented Investigators of Guangdong Province (2021QN020533), the Special Funds of the National Natural Science Foundation of China (82441046), and the Project of Shanghai Institute of Materia Medica, Chinese Academy of Sciences (No. SIMM0120231001) for their financial support.

Appendix A. Supplementary data

Supplementary data to this article can be found online at https://doi.org/10.1016/j.bmcl.2025.130282.

Data availability

Data will be made available on request.

References

1. Pylayeva-Gupta Y, Grabocka E, Bar-Sagi D. RAS oncogenes: weaving a tumorigenic web. *Nat Rev Cancer*. 2011;11:761–774. https://doi.org/10.1038/nrc3106.
2. Hunter JC, Manandhar A, Carrasco MA, Gurbani D, Gondi S, Westover KD. Biochemical and structural analysis of common cancer-associated KRAS mutations. *Mol Cancer Res*. 2015;13(9):1325–1335. https://doi.org/10.1158/1541-7786.mcr-15-0203.
3. Gentile DR, Rathinaswamy MK, Jenkins ML, et al. Ras binder induces a modified switch-II pocket in GTP and GDP states. *Cell Chem Bio*. 2017;24:1455–1466. https://doi.org/10.1016/j.chembiol.2017.08.025.
4. Bar-Sagi D, Knelson EH, Sequist LV. A bright future for KRAS inhibitors. *Nat Can*. 2020;1:25–27. https://doi.org/10.1038/s43018-019-0016-8.
5. Ostrem JM, Peters U, Sos ML, Wells JA, Shokat KM. K-Ras(G12C) inhibitors allosterically control GTP affinity and effector interactions. *Nature*. 2013;503:548–551. https://doi.org/10.1038/nature12796.
6. Ostrem JM, Shokat KM. Direct small-molecule inhibitors of KRAS: from structural insights to mechanism-based design. *Nat Rev Drug Discov*. 2016;15:771–785. https://doi.org/10.1038/nrd.2016.139.
7. Canon J, Rex K, Saiki AY, et al. The clinical KRAS(G12C) inhibitor AMG 510 drives anti-tumour immunity. *Nature*. 2019;575:217–223. https://doi.org/10.1038/s41586-019-1694-1.
8. Lanman BA, Allen JR, Allen JG, et al. Discovery of a covalent inhibitor of $KRAS^{G12C}$ (AMG 510) for the treatment of solid tumors. *J Med Chem*. 2020;63:52–65. https://doi.org/10.1021/acs.jmedchem.9b01180.
9. Hallin J, Engstrom LD, Hargis L, et al. The $KRAS^{G12C}$ inhibitor MRTX849 provides insight toward therapeutic susceptibility of KRAS-mutant cancers in mouse models and patients. *Cancer Discov*. 2020;10:54–71. https://doi.org/10.1158/2159-8290.cd-19-1167.
10. Janes MR, Zhang J, Li LS, et al. Targeting KRAS mutant cancers with a covalent G12C-specific inhibitor. *Cell*. 2018;172:578–589. https://doi.org/10.1016/j.cell.2018.01.006.
11. Song Z, Lou L, Fan G, et al. Identification of novel Pyrrolo[2,3-d]pyrimidine-based KRAS G12C inhibitors with anticancer effects. *Eur J Med Chem*. 2023;245, 114907. https://doi.org/10.1016/j.ejmech.2022.114907.
12. Hofmann MH, Gerlach D, Misale S, Petronczki M, Kraut N. Expanding the reach of precision oncology by drugging all KRAS mutants. *Cancer Discov*. 2022;12(4):924–937. https://doi.org/10.1158/2159-8290.cd-21-1331.

13. Zheng Q, Peacock DM, Shokat KM. Drugging the next undruggable KRAS allele-Gly12Asp. *J Med Chem*. 2022;65(4):3119–3122. https://doi.org/10.1021/acs.jmedchem.2c00099.
14. Bannoura SF, Khan HY, Azmi AS. KRAS G12D targeted therapies for pancreatic cancer: has the fortress been conquered? *Front Oncol*. 2022;12:1013902. https://doi.org/10.3389/fonc.2022.1013902.
15. Lv XD, Lu X, Cao J, et al. Modulation of the proteostasis network promotes tumor resistance to oncogenic KRAS inhibitors. *Science*. 2023;381:1065–1083. https://doi.org/10.1126/science.abn4180.
16. Awad MM, Liu S, Rybkin II, et al. Acquired resistance to KRASG12C inhibition in cancer. *N Engl J Med*. 2021;384(25):2382–2393. https://doi.org/10.1056/nejmoa2105281.
17. Vigil D, Cherfils J, Rossman KL, Der CJ. Ras superfamily GEFs and GAPs: validated and tractable targets for cancer therapy? *Nat Rev Cancer*. 2010;10(12):842–857. https://doi.org/10.1038/nrc2960.
18. Ramharter J, Kessler D, Ettmayer P, et al. One atom makes all the difference: getting a foot in the door between SOS1 and KRAS. *J Med Chem*. 2021;64:6569–6580. https://doi.org/10.1021/acs.jmedchem.0c01949.
19. Jeng HH, Taylor LJ, Bar-Sagi D. Sos-mediated cross-activation of wild-type Ras by oncogenic Ras is essential for tumorigenesis. *Nat Commun*. 2012;3:1168–1175. https://doi.org/10.1038/ncomms2173.
20. Kessler D, Gerlach D, Kraut N, McConnell DB. Targeting son of sevenless 1: the pacemaker of KRAS. *Curr Opin Chem Biol*. 2021;62:109–118. https://doi.org/10.1016/j.cbpa.2021.02.014.
21. Winter JJG, Anderson M, Blades K, et al. Small molecule binding sites on the ras:sos complex can be exploited for inhibition of Ras activation. *J Med Chem*. 2015;58:2265–2274. https://doi.org/10.1021/jm501660t.
22. Hodges TR, Abbott JR, Little AJ, et al. Discovery and structure-based optimization of benzimidazole-derived activators of SOS1-mediated nucleotide exchange on RAS. *J Med Chem*. 2018;61(19):8875–8894. https://doi.org/10.1021/acs.jmedchem.8b01108.
23. Chen T, Tang X, Wang Z, et al. Inhibition of son of Sevenless homologue 1 (SOS1): promising therapeutic treatment for KRAS-mutant cancers. *Eur J Med Chem*. 2023;261, 115828. https://doi.org/10.1016/j.ejmech.2023.115828.
24. Zhang S, Zhang Y, Chen X, et al. Design and structural optimization of orally bioavailable SOS1 inhibitors for the treatment of KRAS-driven carcinoma. *J Med Chem*. 2022;65:15856–15877. https://doi.org/10.1021/acs.jmedchem.2c01517.
25. Ketcham JM, Haling J, Khare S, et al. Design and discovery of MRTX0902, a potent, selective, brain-penetrant, and orally bioavailable inhibitor of the SOS1:KRAS protein−protein interaction. *J Med Chem*. 2022;65:9678–9690. https://doi.org/10.1021/acs.jmedchem.2c00741.
26. Zheng L, Zhang Y, Mei S, et al. Discovery of a potent dual son of Sevenless 1 (SOS1) and epidermal growth factor receptor (EGFR) inhibitor for the treatment of prostate cancer. *J Med Chem*. 2024;67(9):7130–7145. https://doi.org/10.1021/acs.jmedchem.3c02433.
27. Wang Q, Ma F, Wang J, et al. Antitumor activity and transcriptome sequencing (RNA-seq) analyses of hepatocellular carcinoma cells in response to exposure triterpene-nucleoside conjugates. *Eur J Med Chem*. 2024;276, 116635. https://doi.org/10.1016/j.ejmech.2024.116635.
28. Lin L, Marchant RE, Kottke-Marchant K. Extracellular matrix-mimetic poly(ethylene glycol) hydrogels engineered to regulate smooth muscle cell proliferation in 3-D. *Acta Biomater*. 2014;10:5106–5115. https://doi.org/10.1016/j.actbio.2014.08.025.
29. Hillig RC, Sautier B, Schroeder J, et al. Discovery of potent SOS1 inhibitors that block RAS activation via disruption of the RAS-SOS1 interaction. *P Natl Acad Sci USA*. 2019;116(7):2551–2560. https://doi.org/10.1073/pnas.1812963116.